

Cold-rolled composite in situ $\text{AlFe1.8Ti0.4} - \text{Al}_2\text{O}_3\text{p}$

Miao Jingtao, Doctorate Student of the Foundry and Strengthening Engineering Department¹,
e-mail: miaojtingtao22@gmail.com

A. B. Finkelstein, Doctor of Technical Sciences, Professor of the Foundry and Strengthening Engineering Department¹,
e-mail: avinkel@mail.ru

A. A. Shefer, Candidate of Technical Sciences, Associate Professor of the Foundry and Strengthening Engineering Department¹, e-mail: a.a.shefer@urfu.ru

V. A. Khotinov, Doctor of Technical Sciences, Professor of the Heat Treatment and Metal Physics Department¹,
e-mail: v.a.khotinov@urfu.ru

¹Ural Federal University, Yekaterinburg, Russia.

The technology of oxygen blowing of pre-hydrogenated aluminum alloy melt allows to obtain a composite material in situ, saturated with submicroscopic Al_2O_3 particles. The key factor of the technology is the presence of iron in the melt, which negatively affects the strength of the oxide film, which allows to obtain isotropic particles of aluminum oxide, and not extended films. Until now, the technology was used only for cast products based on silumin AlSi7Fe . It is proposed to use an $\text{Al} - \text{Fe}$ alloy with an iron content above 1.5% for obtaining a composite for cold rolling technology. The alloy is also saturated with titanium due to the introduction of TiH_2 for hydrogenation. As a result, a butterfly-shaped structure is formed in the metal, presumably by the following mechanism: the butterfly body is an Al3Ti intermetallic compound, which precipitates in the melt first and collects oxide particles and iron-containing intermetallic compounds. The composite demonstrates grinding of iron intermetallic compounds at least 3 times relative to the original alloy. The content of the oxide component is 8 times lower than on the initial alloy of the AlSi7Fe system due to a significantly smaller thickness of the oxide film. This leads to a significant reduction in the blowing time, the total duration of melt processing, including hydrogen saturation, was 15 min. The samples were subjected to cold rolling, the foil thickness achieved was 19 μm . The obtained rolled product with a thickness of about 150 μm exceeds the original alloy in mechanical properties ($\sigma_u - 269 \text{ MPa}$ against 174 MPa of the original alloy), and the hot-rolled $\text{AlSi7Fe-Al}_2\text{O}_3\text{p}$ composite ($\sigma_u - 250 \text{ MPa}$).

Key words: composite material, strengthening phase, cold rolling, oxide particle, in situ, mechanical properties.

DOI: 10.17580/nfm.2025.02.03

Introduction

Traditional aluminium alloys contain strengthening intermetallic phases. Research in this area suggests that grinding the structure can be used to increase strength [1]. Aluminium matrix composites involve a different approach, in which the strengthening phase is not formed from alloy components but is introduced directly into the alloy – this is known as ex situ technology. Aluminium oxide Al_2O_3 and silicon carbide SiC are mainly used as strengthening components in aluminium matrix composites. This technology appeared first chronologically [2] and is now fairly well studied [3]. The main areas of research are aimed at overcoming technological problems, including segregation of the strengthening phase in the melt, low adhesion of the strengthening phase to the matrix metal, and high porosity formed during gas absorption when mixing filler particles into the melt. The latter problem is related to the difficulty of reducing the size of the strengthening phase particles, which is a key advantage of the technology. To solve these problems, researchers propose various strategies.

When using in situ technology, the particles of the strengthening phase are formed directly in the melt as a result of a chemical reaction between the melt and the precursor, which is introduced into the melt. This solves the problems of adhesion, particle grinding and their uniform distribution in the matrix [4, 5].

Previous research by the authors of this paper shows that submicroscopic (150–250 nm) Al_2O_3 particles form in the pre-hydrogenated AlSi7Fe melt when it is purged with oxygen [6]. According to these results, $\gamma\text{-Al}_2\text{O}_3$ is formed when aluminium melt interacts with oxygen [7]. The technological process involves the formation of oxide bubbles during purging, which are then destroyed on the melt mirror. This destruction occurs due to the formation of gaseous suboxides (AlO and Al_2O) on the melt surface instead of solid aluminium oxide. This is achieved by increasing the melt temperature to 1000 °C during hydrogen combustion [8]. A key factor in this technology is the presence of iron in the melt, which negatively affects the strength of the oxide film. The presence of iron in the alloy at a level of at least 0.8% allows isotropic aluminium oxide particles to be obtained, rather than films. Residual

hydrogen is adsorbed on the surface of aluminium oxide, forming non-stoichiometric hydroxide after crystallisation, with the bound hydrogen content reaching 20 ppm, but this does not lead to the formation of gas porosity [9]. However, the improvement in mechanical properties within this technology due to residual hydrogen, which reduces the bond between the strengthening phase and the matrix, is not so great and amounts to about 50% of the original alloy. Al_2O_3 particles also restrict the flow of the melt during crystallisation, which leads to the formation of shrinkage porosity. To eliminate porosity, improve the bond between phase components and, in general, improve the mechanical properties of composites, pressure treatment is used – rolling and forging [10–14].

The presence of silicon in the original alloy (AlSi7Fe) is due to the use of casting technologies. Silicon improves the fluidity of the melt, but practically does not dissolve in solid metal, and after crystallisation, brittle primary silicon crystals are formed, which limit the plasticity of the alloy, preventing cold rolling. However, hot rolling can significantly improve the mechanical properties of the alloy by 25% [15]. Since silicon is not a mandatory component of the original alloy, unlike Fe, the idea is to use the original Al – Fe alloy system to produce a composite using the proposed technology.

Iron is considered a negative impurity in aluminium alloys because it forms brittle needle-shaped Al_3Fe intermetallics and negatively affects corrosion resistance. Nevertheless, iron is a powerful strengthening component, and iron-containing alloys of the 8xxx series are mainly used for the production of foil [16], primarily alloy 8021B according to the standard [17]. The problem with the Al – Fe system is the widely varying density of the components, Fe and Al, which leads to zonal liquidation, as well as the significant size of Al_3Fe intermetallics. To solve these problems, researchers propose methods such as solid-phase mixing – friction stir welding [18], rapid crystallisation with mechanical mixing and intensive plastic deformation [19].

The proposed technology of purging the pre-hydrogenated Al – Fe melt with oxygen solves these problems: mixing in the melt is ensured during purging, and the formation of large Al_3Fe crystals is prevented by reduced diffusion in the melt due to the presence of aluminium oxide. The authors hope to improve the mechanical properties of the rolled composite material both relative to the standard 8021 alloy and relative to the rolled composite of the AlSi7Fe1 – Al_2O_3 system.

Materials and methods

The original alloy belongs to the Al – Fe system. The presence of elements other than silicon leads to the early destruction of the oxide film within the melt's volume rather than on its surface, resulting in oxide porosity [20]. Silicon is excluded for the aforementioned reasons. Therefore, the presence of elements other than iron in the alloy is undesirable. In accordance with EU

standard [17], the EN AW-8021B alloy with a Fe content of 1.1–1.7% best meets the above conditions.

The technology used to prepare the composite material is similar to that described in [21]. Ingots of pure aluminium Al99.7 (RUSAL, Novokuznetsk, Russia) and an AlFe17 alloy (Metallochemical Company LLC, Yekaterinburg, Russia) were used as the original alloy charge. The chemical composition of these materials was examined using a Spectro Midex spectrometer, the results of which are shown in **Table 1**. Three measurements were taken for each sample and the arithmetic mean was calculated.

Table 1

Chemical composition of the charge (mass %, Al-rest)

	Si	Cu	Mg	Zn	Fe	Ti	V
Al99.7	0.062	<0.001	0.002	0.006	0.141	0.003	0.150
AlFe17	0.12	<0.001	0.302	0.090	17.198	0.022	0.065

A total of 530 g (483 g of pure Al99.7 aluminium and 47 g of AlFe17 alloy) was pre-weighed on AND GF-4000 electronic scales with an accuracy of 1 g and placed in a 700 ml corundum crucible. The crucible was then placed in an electric resistance furnace at a set temperature of 750 °C in order to melt the materials in the charge. Heating continued until the materials had melted. Then, 5 g of TiH_2 hydrogenator (Uralinvest LLC, Ufa, Russia), wrapped in a piece of aluminium foil and weighed on AND GR-300 electronic scales with an accuracy of 0.1 mg, was added to the melt with a plunger and thoroughly mixed with a quartz tube. Five minutes after the completion of the intensive combustion of the released hydrogen, oxygen (supplied by Linde-Uraltehgaz OJSC, Yekaterinburg, Russia) with a flow rate of 0.063 m^3/h , as measured by a rotameter, was blown into the melt through a quartz tuyere for ten minutes. Intense slag formation began after the specified time, which served as an indicator to stop the blowing. After removing the slag, the melt was poured into a sand mould. The installation and casting diagram is shown in **Fig. 1**. To enable comparison of the composite material and the original alloy, the latter was melted and poured in the same way, but without hydrogenation and oxygen purging. Intensive manual stirring with a quartz tube was performed before pouring to prevent zonal liquidation during melting of the original alloy. Four melts were carried out: two to obtain cast cylindrical tensile specimens, and two to obtain rolled flat specimens.

Polished sections were prepared from castings of the original alloy and composite rolled samples, and their microstructure was examined using an Olympus GX-51 optical microscope. The chemical composition of the samples was determined using the aforementioned spectrometer. To determine the aluminium oxide content, the samples were dissolved in a mixture of potassium bromide, bromine and ethyl acetate in accordance with GOST 11793.1-90 [22].

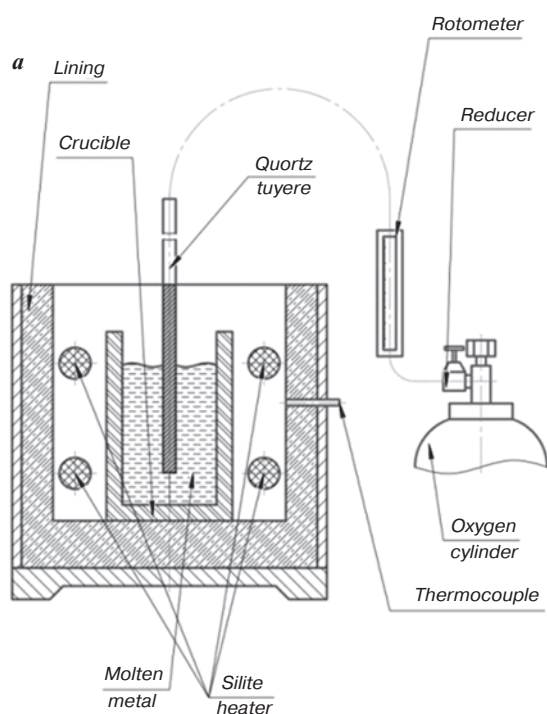


Fig. 1. Installation diagram (a), casting (b)

The samples were mechanically processed to a thickness of 6 mm on a milling machine, cut into three parts (Fig. 2, a) and then rolled on a YUMO B61 electromechanical rolling mill (YUMO-Neva LLC, St. Petersburg, Russia). Rolling was carried out in three stages according to the following scheme: 6 mm – 1 mm – 150 μ m – 20 μ m. Five passes were made at each stage, with a reduction of approximately 20%. Corrections were made at each stage in accordance with the thickness measured using an Inforce 06-11-44 electronic spiral micrometer (Vseinstrumenty.ru LLC, Moscow, Russia; accuracy: 2 μ m).

To study the mechanical properties of rolled stock with an approximate thickness of 150 μ m, samples were

cut using a laser in accordance with GOST 1497–84 [23] in preparation for tensile testing. The samples were then tested for mechanical properties at a speed of 2 mm/min using an Instron 3382 universal testing machine. Three tests were performed on each sample and the arithmetic mean was calculated. Cast cylindrical samples were studied in a similar manner.

Results and discussion

Fig. 2 shows the stages involved in rolling the composite samples. The original alloy samples have a similar appearance. The final thickness of the rolled material is 19 μ m. The absence of cracks at the edges of the rolled

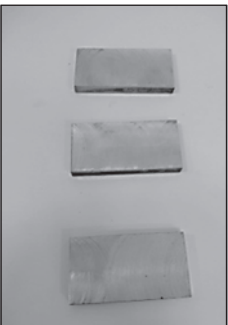
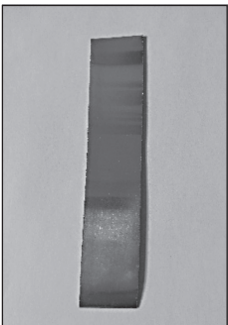


				
	a	b	c	d
Thickness	6 mm	1 mm	160 μ m	19 μ m
Width	30 mm	32 mm	34 mm	37 mm

Fig. 2. Composite rolling stages

material indicates the absence of coarse, brittle intermetallic phases in the composite and original alloy structures (Figs. 3–4).

The composition of the phases is determined by chemical analysis (Table 2).

The Al_2O_3 content in the composite ranges from 0.51% to 0.65% (0.51, 0.57, 0.59, 0.65), with an average of 0.58%.

The significant Ti content in the composite is the result of the dissociation of titanium hydride TiH_2 , which is added to saturate the melt with hydrogen. The solubility limit of titanium in aluminium is 0.024%, and the residual titanium forms the intermetallic compound Al_3Ti [24]. For this reason, titanium is used to refine the structure of aluminium alloys [25]. However, a high concentration of Ti (0.4%) leads to the formation of flat (needle-shaped on the polished section) Al_3Ti crystals up to 300 μm in length [24]. The iron content in the composite was higher than calculated and higher than recommended by the standard for alloy EN AW-8021B, obviously due to zonal liquation in the alloying agent used.

Microstructural analysis shows that both materials are dense, with no porosity, cracks, or other structural defects. The crystals of iron-containing intermetallic compounds are distributed in the structure of the original alloy along the grain boundaries of the aluminium matrix and have an isotropic, rod-like shape. There are no coarse needle-like inclusions, and the phase size does not exceed 10 μm (Fig. 3, b). This structure is characteristic of Al – Fe alloys [25]. Compared to the original alloy, the microstructure of the composite (Fig. 4, a) has structural elements in the form of a butterfly in which the matrix contains a rod-shaped intermetallic phase up to 30 μm long, around which another phase is distributed.

Considering:

- the length of iron-containing intermetallics in the structure of the original alloy is smaller;
- the composite contains aluminium oxide, which limits the growth of phase components;
- the length of the crystals of the Al_3Ti intermetallic phase with a titanium content of 0.4% is up to 300 μm .
- the observed content of the iron-containing intermetallic phase in the composite is significantly lower than in the original alloy.

It can be concluded that the large intermetallic phase in the composite (the body of the butterfly) is Al_3Ti . The surrounding volume (the wings of the butterfly) has a lighter structure due to its saturation with iron intermetallics, which are significantly smaller in size (up to 3 μm), than those in the original alloy (Fig. 4, b). Al_2O_3 particles (less than 250 nm in size [6]) are evenly distributed throughout the metal and refine the structure. The reason for the formation of the butterfly structure is presumably related to the sequence of formation of the phase components: Al_3Ti collects around itself the oxides and iron-containing intermetallics present in the melt, which precipitate from the melt during flow and crystallisation. Despite the relatively large Al_3Ti crystals, cold rolling of the composite is not problematic as these crystals are destroyed by the presence of oxide particles of significantly greater hardness in the structure. This effect even allows rolling of a similar composite based on silumin [15].

The mechanical properties of cast samples of the original alloy and composite are given in Table 3.

The mechanical properties of the original cast alloy correspond to, and even slightly exceed, the results obtained in [27]. This is due to the active mixing of the melt, which prevents iron liquation and reduces the length of needle-like iron intermetallics (see Fig. 3, b).

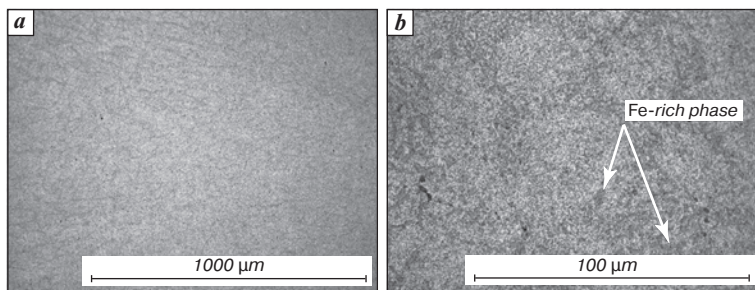


Fig. 3. Microstructure of the original alloy:
a – magnification $\times 100$; b – magnification $\times 1000$

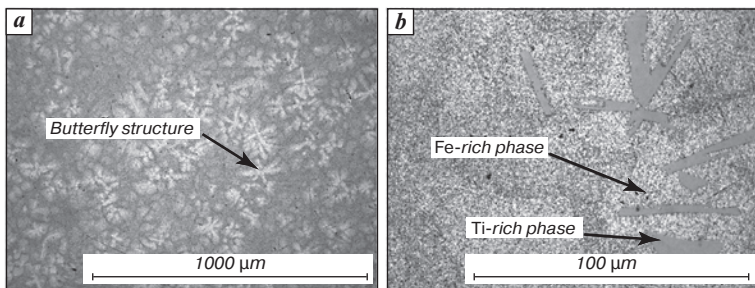


Fig. 4. Microstructure of the composite:
a – magnification $\times 100$; b – magnification $\times 1000$

Table 2

Chemical analysis of alloy and composite

	Si	Cu	Mg	Zn	Fe	Ti	V
Samples for rolling							
Original	0.218	0.015	0.008	0.009	1.151	0.013	0.150
Composite	0.218	0.016	0.019	0.013	1.843	0.468	0.012
Cast samples for mechanical testing							
Original	0.184	0.040	0.022	0.011	1.582	0.002	0.090
Composite	0.266	0.031	0.115	0.006	1.719	0.392	0.065

Compared to the original alloy, the cast composite exhibits a slight increase in strength and a more significant increase in the relative elongation. The composite's higher strength is associated with the contribution of dispersed Al_2O_3 particles to the dispersion of the structure, the difficulty of dislocation slip and the grinding of iron intermetallics. At the same time, the absence of embrittlement by lamellar Al_3Ti inclusions is explained by the formation of “butterfly” structures around these inclusions in the composite. These structures collect oxide inclusions and iron intermetallics, thereby reducing their concentration in the rest of the volume. This is also evidenced by the significant dispersion of relative elongation and yield strength. The slight increase in the composite's strength properties is due to the samples rupturing outside the high-strength ‘butterfly’ structures, which have a lower concentration of strengthening phases.

The mechanical properties of the composite obtained are slightly lower than those reported in work [28], in which a cast $\text{AlFe1.7} - \text{Al}_2\text{O}_3$ composite was produced by mixing 50 μm diameter electrolytic iron microspheres into molten aluminium. In this work, aluminium oxide was formed as a result of an aluminothermic reaction on the surface of the microspheres, a fact that was not identified by the authors. However, its presence is evident from the significant improvement in the tribological characteristics of the composite. The higher mechanical properties observed in [28] are due to the absence of the embrittling effect of titanium intermetallics. Using the proposed composite production technology did not significantly increase the mechanical properties of the cast AlFe1.5 alloy, as was observed with the cast AlSi7Fe [14], since there are fewer phase components that are ground by the presence of aluminium oxide, and less aluminium oxide itself was formed, not 4–5%, but 0.5–0.6%. This decrease in the aluminium oxide mass fraction is associated with a decrease in the oxide film thickness on aluminium-iron alloys [29]. Consequently, the aluminium oxide particles formed by implementing the technology have a large specific surface area. This leads to a significant reduction in the time required for oxygen blowing of the melt, as observed experimentally. The duration of blowing is determined by the residual hydrogen, which maintains the temperature of the melt mirror at a level sufficient for the formation of gaseous aluminium suboxides during combustion. Hydrogen is also adsorbed onto aluminium oxide particles [30]. The end of the blowing process is identified visually when slag covers the melt mirror. For the AlSi7Fe alloy, the duration of blowing at the same specific oxygen consumption was about one hour, and for the $\text{Al} - \text{Fe}$ alloy system, it was 10 minutes.

However, pressure treatment is a reserve for improving the mechanical properties of the AlFe1.5 -based composite, which, although possible for the cast AlSi7Fe alloy, is extremely technologically unfeasible [15]. The

Table 4

Mechanical properties of rolled original alloy and composite

Material	Degree of deformation	σ_u , MPa	$\sigma_{0.2}$, MPa	δ , %
Original alloy	~40	174.0 ± 4.8	167.0 ± 3.8	3.3 ± 0.9
Composite	~7	201.0 ± 11.0	180.0 ± 7.8	5.0 ± 0.5
	~40	269.0 ± 7.8	242.0 ± 6.4	3.2 ± 0.3

results of mechanical tests of the rolled original alloy and composite are given in Table 4.

The mechanical properties of the rolled alloy are consistent with the data in [30]. The significant improvement in the composite's mechanical properties relative to the original alloy can be explained by an increased proportion of strengthening phases: the composite contains slightly higher proportions of iron (1.8% versus 1.5%), titanium (0.4%) and aluminium oxide (0.6%). However, aluminium oxide is not the main strengthening component of the alloy. However, its presence inhibits diffusion, preventing the needle-like phases from growing to significant sizes and becoming stress concentrators. As is clear from the results of work [15], during rolling the harder aluminium oxide causes Al_3Ti to be crushed, resulting in a homogeneous distribution of strengthening phases throughout the alloy volume. This can be seen from the relative elongation, which is close in magnitude to that of the initial alloy, and the minimum dispersion of relative elongation. Homogenisation of the structure during rolling enables the full realisation of the dispersion strengthening mechanism, in contrast to the cast alloy.

Titanium aluminide is an important strengthening phase. Introducing titanium into the gas-forming phase ensures its uniform distribution throughout the metal volume [32]. The isolated introduction of hydride leads to the formation of foam metal, which is the standard production technology [33]. Oxygen blowing is necessary to eliminate porosity. Significantly greater refinement of the structure, and consequently an increase in the mechanical properties of deformed $\text{Al} - \text{Fe}$ alloys, can be achieved through intensive plastic deformation; however, this process is much more expensive [34].

Thus, the proposed technology enables the production of a strong aluminium alloy with a foil thickness of 19 μm through cold rolling and short-term modification treatment, namely:

- introduction of titanium into TiH_2 ;
- oxygen blowing for 10 minutes.

Conclusions

The adaptation of technology to obtain a composite material in situ by blowing oxygen into a pre-hydrogenated melt of an $\text{Al} - \text{Fe}$ alloy system, followed by pressure treatment, showed that:

- due to the saturation of the melt with titanium introduced into TiH_2 for hydrogenation, a “butterfly” structure is formed in the metal;

- the structural components of the strengthening phases are refined by at least three times;
- the composite exhibits an oxide component content eight times lower than that of the initial AlSi7Fe alloy, due to the significantly lower thickness of the oxide film. This also leads to a significant reduction in purging time: the total duration of melt processing, including hydrogen saturation, was 15 minutes;
- during cold rolling of the composite, a foil thickness of 19 μm was achieved;
- the resulting rolled product has improved mechanical properties compared to the original alloy ($\sigma_u = 269$ MPa versus 174 MPa for the initial alloy) and the hot-rolled AlSi7Fe – Al₂O₃p composite ($\sigma_u = 250$ MPa).

References

1. Friedlaender I. N. Aluminum and Its Alloys. Moscow: Znanie, 1965. 62 p.
2. Handbook of composites. Ed. by Lubin G. New York: Springer Science + Business Media, LLC, 1982. 786 p.
3. Singh J., Chauhan A. Characterization of Hybrid Aluminium Matrix Composites for Advanced Applications – a Review. *Journal of Materials Research and Technology*. 2016. Vol. 5, Iss. 2. pp. 159–169.
4. Wang H., Li G., Zhao Y., Chen G. In Situ Fabrication and Microstructure of Al₂O₃ Particles Reinforced Aluminum Matrix Composites. *Materials Science and Engineering: A*. 2010. Vol. 527, Iss. 12. pp. 2881–2885.
5. Chen B., Zhou X. Y., Zhang B., Kondoh K., Li J. S., Qian M. Microstructure, Tensile Properties and Deformation Behaviors of Aluminium Metal Matrix Composites Co-Reinforced by Ex-Situ Carbon Nanotubes and In-Situ Alumina Nanoparticles. *Materials Science and Engineering: A*. 2020. Vol. 795. 139930.
6. Chikova O. A., Finkel'shtein A. B., Shefer A. A. Structure and Nanomechanical Properties of the Al–Si–Fe Alloy Produced by Blowing the Melt with Oxygen. *Physics of Metals Metallography*. 2018. Vol. 119. pp. 685–690.
7. Bonner S. J., Taylor J. A., Yao J.-Y., Rhamdhanil M. A. Oxidation of Commercial Purity Aluminum Melts: an Experimental Study. In: *Light Metals 2013* (Ed. by Sadler B. A.). pp. 993–997.
8. Finkelstein A., Schaefer A., Chikova O., Borodianskiy K. Study of Al – Si Alloy Oxygen Saturation on Its Microstructure and Mechanical Properties. *Materials*. 2017. Vol. 10, Iss. 7. pp. 786–793.
9. Finkelstein A. B., Chikova O. A., Shefer A. A., Makhmudzoda M. Oxydal – a New Aluminium Composite. *Liteinoye Proizvodstvo*. 2019. Iss. 7. pp. 6–8.
10. Lokesh G. N., Ramachandra M., Mahendra K. V. Effect of Hot Rolling on Al – 4.5% Cu Alloy Reinforced Fly Ash Metal Matrix Composite. *International Journal of Composite Materials*. 2014. Vol. 4, Iss. 1. pp. 21–29.
11. Kumar S. A., Shekhar P. S., Krushna M. G. Effect of Hot Rolling on Physical and Mechanical Properties of Al 6061 Alloy-Based Metal Matrix Composite. In: *Advances in Mechanical Processing and Design* (Eds. by Pant P., Mishra S. K., Mishra P. C.). 2019. pp. 319–330.
12. Afkham Y., Khosroshahi R. A., Rahimpour S., Aavani C., Brabazon D., Mousavian R. T. Enhanced Mechanical Properties of in Situ Aluminium Matrix Composites Reinforced by Alumina Nanoparticles. *Archives of Civil and Mechanical Engineering*. 2018. Vol. 18. pp. 215–226.
13. Ceschini L., Minak G., Morri A. Forging of the AA2618/20 vol.% Al₂O₃p Composite: Effects on Microstructure and Tensile Properties. *Composites Science and Technology*. 2009. Vol. 69, Iss. 11–12. pp. 1783–1789.
14. Khosroshahi N. B., Mousavian R. T., Khosroshahi R. A., Brabazon D. Mechanical Properties of Rolled A356 Based Composites Reinforced by Cu-Coated Bimodal Ceramic Particles. *Materials & Design*. 2015. Vol. 83. pp. 678–688.
15. Finkelstein A. B., Pellenen A. P., Khotinov V. A., Miao Jingtao. Hot Rolling of the Composite Manufactured by Oxygen Lancing of AlSi7Fe Melt. *Tsvetnye Metally*. 2024. No. 3. pp. 34–39.
16. Kraner J., Smolar T., Volšak D., Lažeta M., Skrbinek R., Fridrih D., Cvahte P., Godec M., Paulin I. Influence of the Hot-Rolling Technique for En Aw-8021B Aluminium Alloy on the Microstructural Properties of a Cold-Rolled Foil. *Materials and Technology*. 2021. Vol. 55, Iss. 6. pp. 773–779.
17. DIN EN 573–3–2009. Aluminium and Aluminium Alloys – Chemical Composition and Form of Wrought Products – Part 3: Chemical Composition and Form of Products. 2009. 32 p.
18. Lee I. S., Kao P. W., Ho N. J. Microstructure and Mechanical Properties of Al – Fe in Situ Nanocomposite Produced by Friction Stir Processing. *Intermetallics*. 2008. Vol. 16, Iss. 9. pp. 1104–1108.
19. Kaloshkin S. D., Tcherdyntsev V. V., Tomilin I. A., Gunderov D. V., Stolyarov V. V., Baldokhin Y. V., Brodova I. G., Shelekhov E. V. Composed Phases and Microhardness of Aluminium-Rich Aluminium-Iron Alloys Obtained by Rapid Quenching, Mechanical Alloying and High-Pressure Torsion Deformation. *Materials Transactions*. 2002. Vol. 43, Iss. 8. pp. 2031–2038.
20. Finkelstein A., Schaefer A., Dubinin N. Aluminum Alloy Selection for In Situ Composite Production by Oxygen Blowing. *Metals*. 2021. Vol. 11, Iss. 12. 1984.
21. Finkelstein A., Schaefer A., Dubinin N. Dehydrogenation of AlSi7Fe1 Melt during In Situ Composite Production by Oxygen Blowing. *Metals*. 2021. Vol. 11, Iss. 4. 551.
22. GOST 11739.1–90. Aluminium Casting and Wrought Alloys. Methods for Determination of Aluminium Oxide. Moscow: Gosudarstvenniy Komitet SSSR po Upravleniyu Kachestvom Produktov i Standartam, 1990. 12 p.
23. GOST 1497–84. Metals. Methods of Tension Test. Moscow: Standartinform, 2008. 22 p.
24. Wang F., Eskin D., Mi J., Connolley T., Lindsay J., Mounib M. A Refining Mechanism of Primary Al₃Ti Intermetallic Particles by Ultrasonic Treatment in the Liquid State. *Acta Materialia*. 2016. Vol. 116. pp. 354–363.
25. Jaradeh M., Carlberg T. Effect of Titanium Additions on the Microstructure of DC-Cast Aluminium Alloys. *Materials Science and Engineering: A*. 2005. Vol. 413. pp. 277–282.

26. Seikh A. H., Baig M., Singh J. K., Mohammed J. A., Luqman M., Abdo H. S., Khan A. R., Alharthi N. H. Microstructural and Corrosion Characteristics of Al-Fe Alloys Produced by High-Frequency Induction-Sintering Process. *Coatings*. 2019. Vol. 9, Iss. 10. 686.
27. Wang W., Sun Q., Zhang K. Modification Mechanism and Mechanical Properties of 8021 Aluminum Alloys. *Journal of Materials Engineering and Perform.* 2025. DOI: 10.1007/s11665-025-10851-0.
28. Srivastava S., Mohan S. Study of Wear and Friction of Al – Fe Metal Matrix Composite Produced by Liquid Metallurgical Method. *Tribology in Industry*. 2011. Vol. 33, Iss. 3. pp. 128–137.
29. Hinton E. M., Griffiths W. D., Green N. R. Comparison of Oxide Thickness of Aluminium and the Effects of Selected Alloying Additions. *Materials Science Forum*. 2013. Vol. 765. pp. 180–184.
30. Braaten O., Kjekshus A., Kvande H. The Possible Reduction of Alumina to Aluminum Using Hydrogen. *JOM*. 2000. Vol. 52, Iss. 2. pp. 47–53.
31. Fuxiao Y., Fang L., Dazhi Z., Toth L. S. Microstructure and Mechanical Properties of Al – 3Fe Alloy Processed by Equal Channel Angular Extrusion. *IOP Conference Series: Materials Science and Engineering*. 2014. Vol. 63, Iss. 1. 012079.
32. Pat. SU No. 551390 A1. Int. Cl. C22, C1/10. The Method of Modifying Aluminum Alloy with Titanium. Pogrebnyak D. A., Tarasova I. V., Polesya A. F. Appl. 18.12.1975, Publ. 25.03.1977.
33. Babcsán N., Leitlmeier D., Degischer H. P., Banhart J. The Role of Oxidation in Blowing Particle–Stabilised Aluminium Foams. *Advanced Engineering Materials*. 2004. Vol. 6, Iss. 6. pp. 421–428.
34. Cubero-Sesin J. M., Horita Z. Strengthening of Al Through Addition of Fe and by Processing with High-Pressure Torsion. *Journal of Materials Science*. 2012. Vol. 48. pp. 4713–4722. 